Optical cavities and quantum emitters

Koks, C.

Summary

This thesis describes steps towards creating a good single-photon source. To achieve this, we need a good single-photon emitter and a good optical resonator. This thesis mainly focuses on the study of the microcavity resonator (chapters 2-6) and ends with a chapter on quantum emitters in hexagonal Boron Nitride (chapter 7). The main finding of this thesis is that good cavities, i.e. those with many reflections and strongly confined modes, exhibit significant deviations from the standard theory of optical cavities. These deviations are thoroughly investigated in this thesis.

Figures S.1a and S.1b illustrate the working principle of the Fabry-Perot cavity resonator. Two highly-reflective mirrors are placed closely together. For one mirror, almost all light reflects and only a tiny portion of the light is transmitted. The magic of the Fabry-Perot cavity is that when a second mirror is added, all of the light can be transmitted. The requirement is that the optical mode should fit precisely between the two mirrors, as is the case in Fig. S.1b. When this happens, all the tiny fractions of light that get transmitted through the second mirror interfere constructively and add up to unity. This is schematically illustrated in Fig. S.1b by the red and blue arrows with positive and negative phases respectively. All light on the right side of the two mirrors has the same phase and thus adds up. The initial reflected beam on the left side is in anti-phase with all transmitted light through the left mirror and sums up to zero. Hence, at resonance, we can measure a peak in transmission and a dip in reflection.

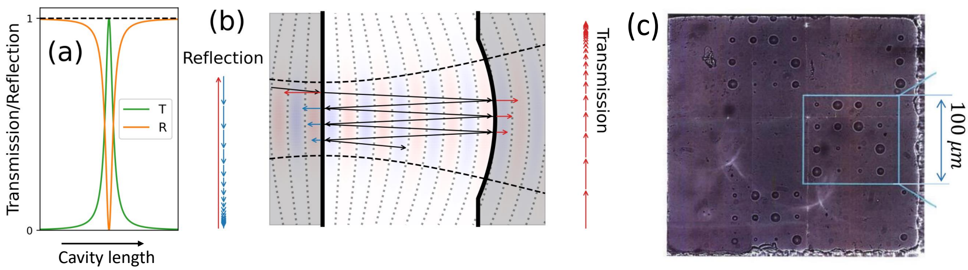

Figure S.1: (a) Transmission and reflection spectra of an ideal Fabry-Perot cavity. At resonance, all light is transmitted and no light is reflected. (b) Sketch of a plano-concave Fabry-Perot cavity. The two solid black lines show the mirrors, where the right mirror is a micromirror with a dimple with very small radius of curvature which matches the wavefronts (dotted lines). The arrows sketch the many reflections of the light, with blue and red being in opposite phase. The colored (light blue/red) blobs show the electric field amplitude between the two mirrors. The two black dashed lines follow the strongly diverging opening angle of the mode. (c) Wide-field microscopy image of the micromirrors. The circles are dimples in the mirror with radii of curvature $R \approx 25$ μm for the biggest circles and $R \approx 3$ μm for the smallest circles.

From the cavity lengths at which the resonances occur, we can deduce the shape of the optical mode with very high accuracy, down to 25 picometers, which is half the size of a hydrogen atom. The shape can deviate from the standard theory when the mode is strongly focused and the opening angle is large. The deviation is illustrated by the mismatch between the wavefront (dotted curves) and mirror (solid spherical curve) in Fig. S.1b. These large opening angles naturally occur when micromirrors are used for the cavity.

Figure S.1c shows the micromirrors that are used in this thesis. These micromirrors are fabricated by Oxford HighQ (UK) by creating little dimples in a glass slide using a focused ion beam, which are then coated with reflective material. These dimples have radii of curvature between 3 and 25 μm and diameters between 2 to 10 μm. This is the same size as some bacteria, or more importantly, the size of only a few optical wavelengths λ. When the radius of curvature of the mirror $R \lesssim 10\lambda$, the conventional paraxial description of the cavity modes breaks down and nonparaxial effects have to be taken into account.

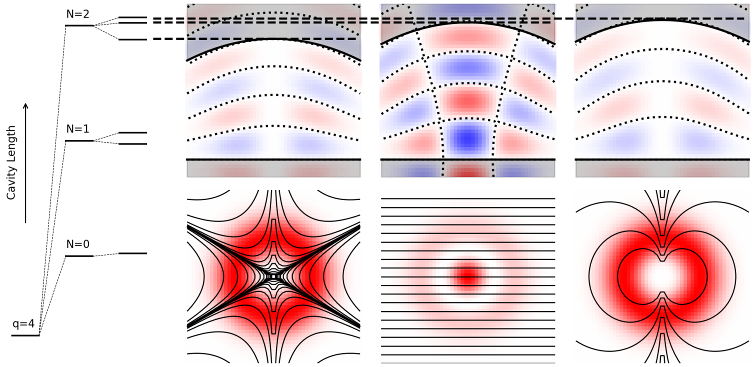

Figure S.2: Schematic figure to show cavity lengths at which certain modes are resonant. (left) Graph of fine structure splittings, similar to those found in textbooks on quantum mechanics. (right) Three modes of the $N = 2$ transverse mode group all have slightly different resonant cavity lengths, according to nonparaxial theory. The images are not to scale.

Figure S.2 schematically shows the resonance spectrum of a microcavity. The transverse modes labeled $N = 1$ and $N = 2$ split up because of the unavoidable nonparaxial effects in the microcavity. The spatial profiles in the length and transverse direction for the $N = 2$ mode group are illustrated on the right in Fig. S.2, where the length of each of the three modes is slightly different. The three modes have a distinct field distribution (red and blue colors) and polarization profile (black lines in the bottom figure). The flower-like polarization profiles of the left and right modes are a consequence of spin-orbit coupling, which causes their splitting. The central mode is not affected by spin-orbit coupling but is shifted in cavity length with respect to the center of the two modes because it reflects from a different part of the mirror. We call the splitting of peaks due to unavoidable nonparaxial effects a “fine structure”. The fine structure is fundamental to microcavities, meaning it cannot be removed by making better mirrors.

The fine structure becomes prominent in the resonance spectra when the finesse F is high and the relative radius of curvature R/λ is small. Other effects, like penetration depth and mode-mixing, also become increasingly important when $F\lambda/R$ increases. Coincidentally, cavities with strong light-matter interaction also have a large factor $F\lambda/R$. The cavity used in the research here is a fairly regular microcavity and the literature reports microcavities with much larger factors $F\lambda/R$. We believe that many of the effects described in this thesis must also have been observed by other research groups, but they were not reported on in detail. In this thesis, we show measurements of these concepts and provide useful working formulas to understand and make use of the many modes in the microcavity.

This thesis consists of 7 chapters. It starts with an introduction chapter and continues with 6 chapters whose contents are summarized below.

Chapter 2 analyzes how light penetrates the highly reflective DBR mirrors. We found that this process can be conveniently described with three penetration depths. Which penetration depth should be used depends on the experiment that is performed. First, the phase penetration depth describes the shift of the (anti-)nodes in or out of the DBR. Second, the frequency penetration depth determines how much a light pulse is delayed due to penetration into the mirror. Last, the modal penetration depth indicates the shift of the focal point when a beam is focused on the mirror. The difference between these penetration depths can be of the order of a wavelength, so it is important to consider this when using microcavities. Our analysis helps other researchers to choose the correct penetration depth to describe their measurements.

Chapter 3 shows measurements of mode-mixing in an optical cavity. This mode-mixing occurs when a fundamental mode and transverse mode are resonant at (almost) the same frequency/cavity length. Mode-mixing is a very widespread concept in physics that is usually measured in the frequency domain. Instead, we measure mode-mixing via the spatial profiles of the eigenmodes, which also mix. This method proves to be much more sensitive such that smaller mixing amplitudes can be observed.

Chapter 4 describes a theory to calculate how nonparaxial effects create a microcavity fine structure. The fine structure can be observed in length or frequency scans as a splitting of resonances that should be degenerate according to the standard paraxial theory. The word “fine structure” is taken from atomic physics, where small splittings were observed which could only be explained by fundamental (relativistic) corrections on the Schrödinger equation. The microcavity fine structure can only be explained by fundamental (nonparaxial) corrections on the paraxial wave equations. The fine structure is unavoidable when microcavities are used, for which we provide useful working formulas to fully describe the resonance spectra.

Chapter 5 shows measurements of the microcavity fine structure. We observe several peaks that we would expect from paraxial theory. But when we zoom in on these peaks, we find splittings that can only be described by nonparaxial theory. Using a polarization-resolving CCD camera, we can label each of the modes, and compare them to theoretical predictions. We find that the nonparaxial theory accurately predicts the splittings. These findings confirm the importance of nonparaxial corrections in optical microcavities.

Chapter 6 demonstrates all the concepts mentioned above (penetration depths, mode-mixing, and fine structure) but now using intracavity emitters instead of an external light source such as a laser or a white light lamp. Using intracavity emitters, we can accurately measure the wavelength and cavity length dependence of all cavity modes. The advantage of this method is that we can now determine the penetration depth without having to rely on a rough estimate of the exact cavity length, and we can now determine the mode-mixing in the frequency domain. The cavity length- and wavelength-dependent intensity maps give a rich insight into all of the unexpected microcavity behavior.

Chapter 7 shows measurements with a home-built confocal microscope on quantum

emitters in hexagonal Boron Nitride (hBN) flakes. We scan the hBN flake and measure many fluorescent centers. Most of them quickly stop emitting light, which limits their usefulness. Only very few centers stayed alive for several hours, during which their dipole orientation, emission spectra, and emission dynamics were measured. We found that the excitation and emission dipoles are not always aligned and that the emitted light bunches with two different, power-dependent, bunching times. Our observations can be used to better identify the emitter and its surroundings.